Supporting information for

Rational design of efficient Pt_3Cu/TiO_2 icosahedra catalysts for bio-aviation fuel production under a mild condition

Yichen Nie [1a, b], Xingyong Li [1*a, b, f], Misbah Uddin[a], Na Liu [a, b], Senshen Yu [a, b], Phidsavard Keomeesay [a, c], Olajide-rasheed Olalekan [a], Shuaizhe Li [a, b], Yubao Chen [**a, b], Xuebing Zhao [***d], Longlong Ma [e], Zhifeng Zheng [f], Shijie Liu [g],

a. School of Energy and Environmental Science, Yunnan Normal University, Kunming, Yunnan, 650500, PR China

b. Key Laboratory of Green Biomass Energy and Platform Compounds, Yunnan Provincial Department of Education; Key Laboratory of Renewable Energy Advanced Materials and Manufacturing Technology，Ministry of Education, Kunming, Yunnan 650500, PR China

c. Louangnamtha Teacher Training college, Louangnamtha Province, 03000, Lao PDR

d. Institute of Applied Chemistry, Department of Chemical Engineering, Tsinghua University, Beijing 100084, PR China

e. Key Laboratory of Energy Thermal Conversion and Control of Ministry of Education, School of Energy and Environment, Southeast University, Nanjing 210096, PR China

f. College of Energy, Xiamen University, Xiamen 361102, China

g. Department of Chemical Engineering, SUNY College of Environmental Science and Forestry, Syearacuse, NY 13210, USA

Co-first author. Both Yichen Nie and Xingyong Li made equal contributions in this work.

Corresponding authors:

Assistant Prof./Dr. Xingyong Li, xingyong@ynnu.edu.cn, Prof./Dr. Yubao Chen,

chenyubao@ynnu.edu.cn, Prof./Dr. Xuebing Zhao, zhaoxb@mail.tsinghua.edu.cn

Characterization conditions：

Powder X-ray diffraction (XRD) was used to characterize the catalysts' phase and structure at 40 kV and 40 mA using nickel-filtered Cu Kα radiation (λ=0.154 nm), covering 2θ from 5° to 90°.

Transmission electron microscopy (TEM) images were obtained using a FEI Talos F200X at 200KV. Take part of the sample dispersed into the ethanol solution for sonication, and then take a few drops of well dispersed liquid added drop by drop on the Cu mesh, after drying, photographed morphology (high-resolution), energy spectra model EDS super-X, photographed energy spectra surface sweep.

Scanning electron microscope (SEM) images were generated using a ZEISS Sigma 300 operated at 15 kV to observe the morphologies of the catalyst. A trace amount of sample was taken and stuck directly onto the conductive adhesive and sprayed with gold for 45 s using a Quorum SC7620 sputtering coater at 10 mA. Subsequently, a scanning electron microscope was used to take photos of the sample morphology and energy spectrum mapping, etc., with an accelerating voltage of 3 kV for morphology shooting and 15kV for energy spectrum mapping, and the detector was a SE2 secondary electron detector.

The textural parameters of the catalysts were analyzed by N_2 sorption isotherms with ASAP 2010 Plus at −196°C. Prior to measurement, the catalyst was degassed under vacuum at 200 °C for 4 h. The BET surface area, pore diameter and pore volume were calculated from the linear part of the BET plot.

The NH_3-TPD characterization was performed by heating 100 mg samples at a rate of 10 °C /min to 200 °C for 1 h in Ar atmosphere, followed by cooling to 80 °C with an Ar gas flow. The NH_3 adsorption flow rate was 30 mL/min for 2 h. The adsorbed NH_3 was removed by heating at a rate of 10 °C /min to 450 °C.

Raman wavelengths 532 nm and 633 nm, exposure time 10S, overlapped twice. Model: Renishaw inVia Qontor. FTIR with potassium bromide as substrate.

X-ray photoelectron spectroscopy (XPS) was performed on a Thermo Fisher Scientific Nexsa spectrometer equipped with a monochromatic Al Kα source. The operating voltage was 15 kV, the operating current was 10 mA, and the samples were analyzed under vacuum (5x10-10 Pa) with a pass energy of 50 eV (roving scan). All peaks were corrected with an indeterminate carbon C1s peak binding energy of 284.8 eV. Spread the sample on the double-sided tape and use a clean sampling spoon to spread the powder evenly and as thinly as possible on the tape. Take another piece of aluminum foil wiped clean with acetone and cover the sample. Place the aluminum foil + sample between two flat stainless steel modules and press the piece together. Remove the aluminum foil covering the sample and gently tap the aluminum foil with the sample to remove any remaining powder from the surface. The aluminum foil was cut around the perimeter of the pressed sample to produce a ~1 cm x 1 cm pressed sample which was placed in the sample stage for testing. Monochromatic Al Ka (hv =1486.6 eV), power 150 W, spot size 400 μm. Test results were corrected for C1s of 284.8 eV. The XPS patterns were fitted using XPSPEAK41 software.

GC-MS conditions: The composition of the liquid products was detected by gas chromatography-mass spectrometry (GC-MS) under the following conditions: GC conditions: CETM-5 column (30 m×0.25 mm×0.25 μm); injection temperature: 250 ℃; temperature increase procedure: initial temperature: 80 ℃, hold for 2 min; heating rate: 5 ℃/min up to 130 ℃; hold for 5 min; heating rate: 5 ℃/min up to 180 ℃; hold for 5 min; heating rate: 5 ℃/min up to 230 ℃; holding for 5 min; carrier gas (He) flow rate: 1.0 mL/min; MS: 1.0 mL/min; carrier gas (He) flow rate: 1.0 mL/min. MS conditions: electron bombardment (EI) ion source (electron energy 70 eV, temperature 250 ℃), transmission line temperature 270 ℃, detection voltage 0.9 kV, mass scan range (m/z) 60 ~ 500, data acquisition time range of 4.20~47.00 min. The relative retention times of the alkane components were determined by GC-MS and compared with the Nist 08 standard spectral library, and the relative contents of the alkane components were obtained by the area normalization method.

XAS analysis was conducted with Si (111) crystal monochromators at the BL13SSW beamlines of the Shanghai Synchrotron Radiation Facility (SSRF) (Shanghai, China). Before the beamline analysis, the samples were compacted into thin sheets with a diameter of 1 cm and sealed using Kapton tape film. The XAFS spectra were recorded at ambient temperature. Extended X-ray absorption fine structure (EXAFS) spectra were recorded in transmission mode or fluorescence mode. Negligible changes in the line shape and peak position of XANES spectra were observed between two scans taken for a specific sample. The XAFS spectra of these standard samples were also recorded in transmission mode or fluorescence mode. All the spectra were analyzed and fitted in Athena and Artemis software packages.

The dissolved metal concentrations were quantified using an Agilent 720ES inductively coupled plasma-optical emission spectrometry (ICP-OES).

The Py-IR experiments were used to calculate the Lewis acid and Bronsted acid contents. The samples were heated with a temperature pro-gram to 250 °C and held for 2 h under vacuum conditions (10-2 pa), followed by cooling to room temperature. The spectra were then recorded in FTIR. Subsequently, the catalysts were exposed to pyridine vapor for 0.5 hours at ambient temperature, and the spectra of the catalysts after pyridine adsorption were obtained. After desorption at temperatures of 150 °C and 250 °C for 1 h, the spectra of the catalysts desorbed at 150 °C and 250 °C were received, respectively. Finally, calculate the content of Lewis acid and Bronsted acid based on the peak area at the corresponding position.

A photothermal catalytic reactor equipped with scratch–resistant sapphire that allows 99% of the incident light to pass through guaranteed that the catalyst could be fully illuminated (Fig. S1); the reactor was designed and manufactured by CEAULIGHT Mechanical Equipment Co Ltd, Beijing, China. The manufacturer's details of the remaining equipment are as follows: CEL–HXF300–T3 xenon lamp system was employed to simulate solar light (radiant output: 50 W, UV output: 2.6 W, IR output: 28.8 W, visible output: 5000 lm, spectral output: 320–2500 nm).

.

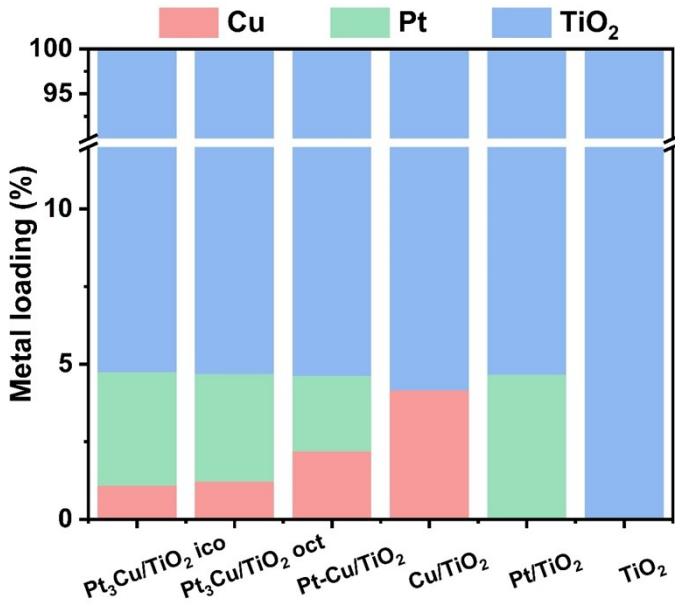

Fig. S1. The ICP-OES results of catalysts.

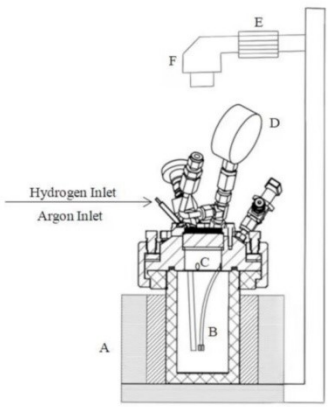

A. control panel and heating element; B. reaction tank; C. scratch–resistant sapphire window; D. pressure meter; E. xenon lamp system; F. retroreflector;

Fig. S2. A schematic diagram of the photothermal reactor.

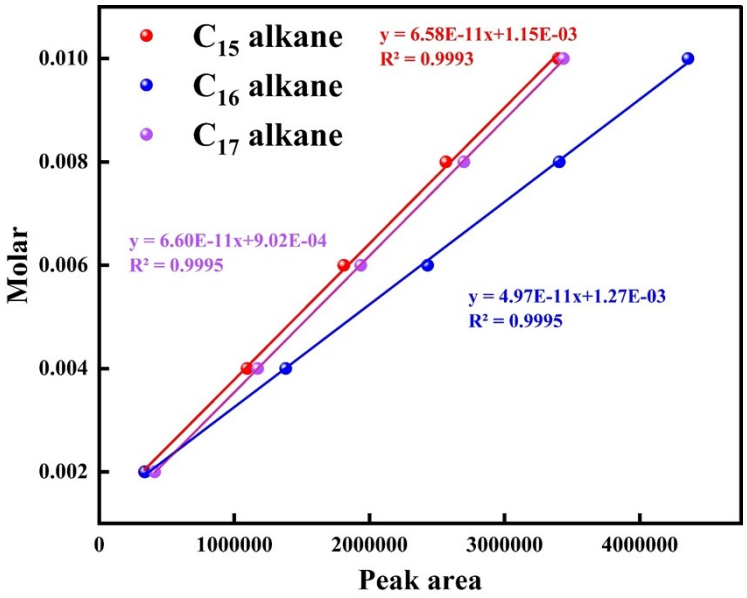

Fig. S3. The external standard curves of C_{15}-C_{17} alkanes.

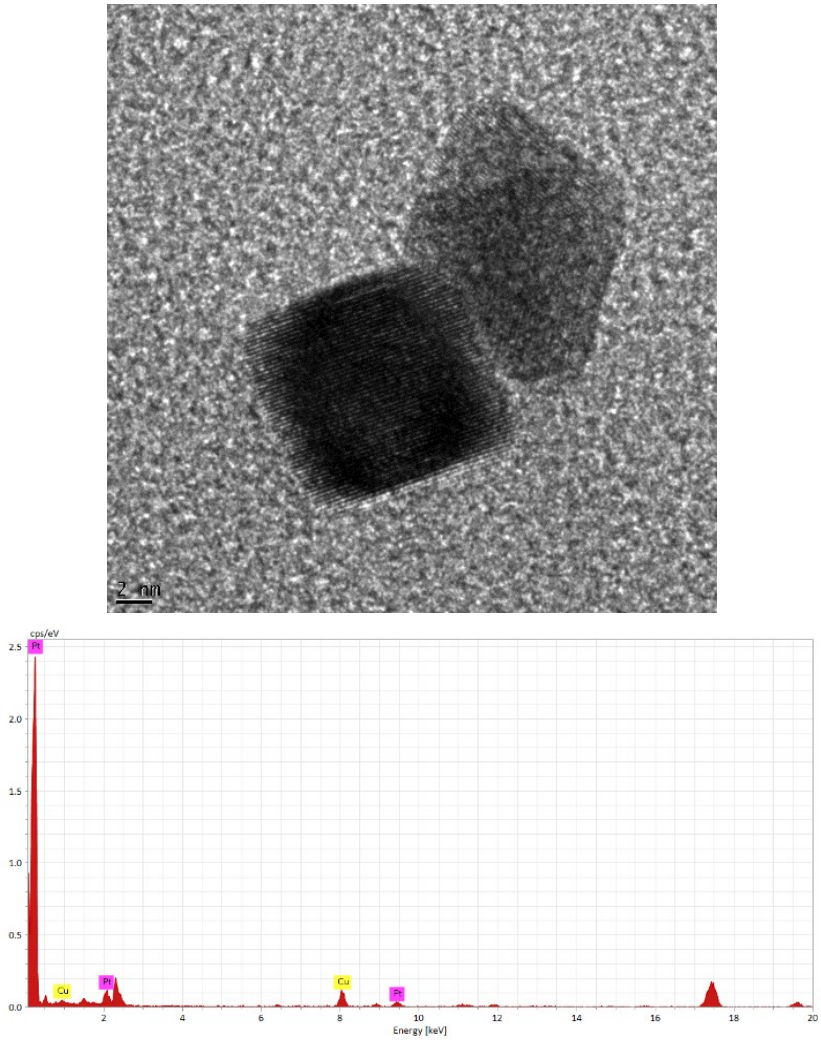

Fig. S4. TEM image of Pt_3Cu oct.

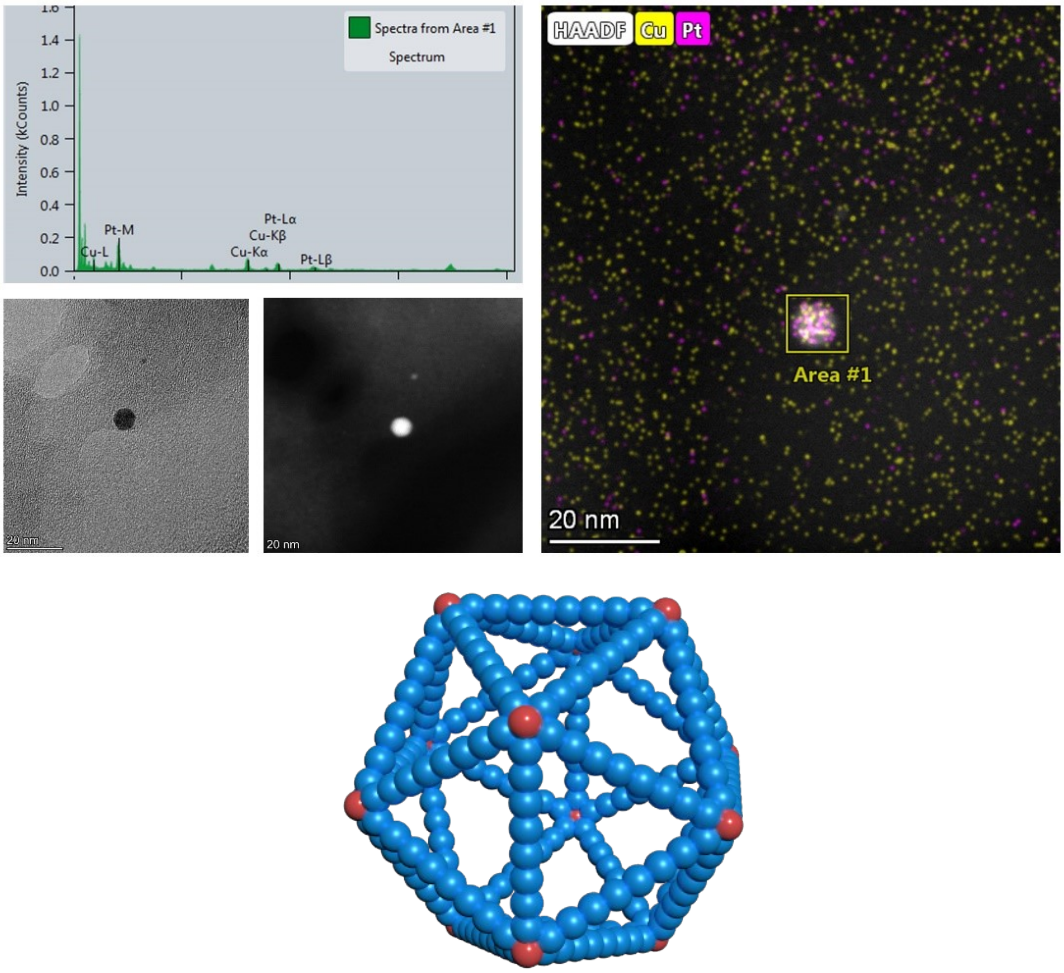

Fig. S5. TEM images of Pt_3Cu ico.

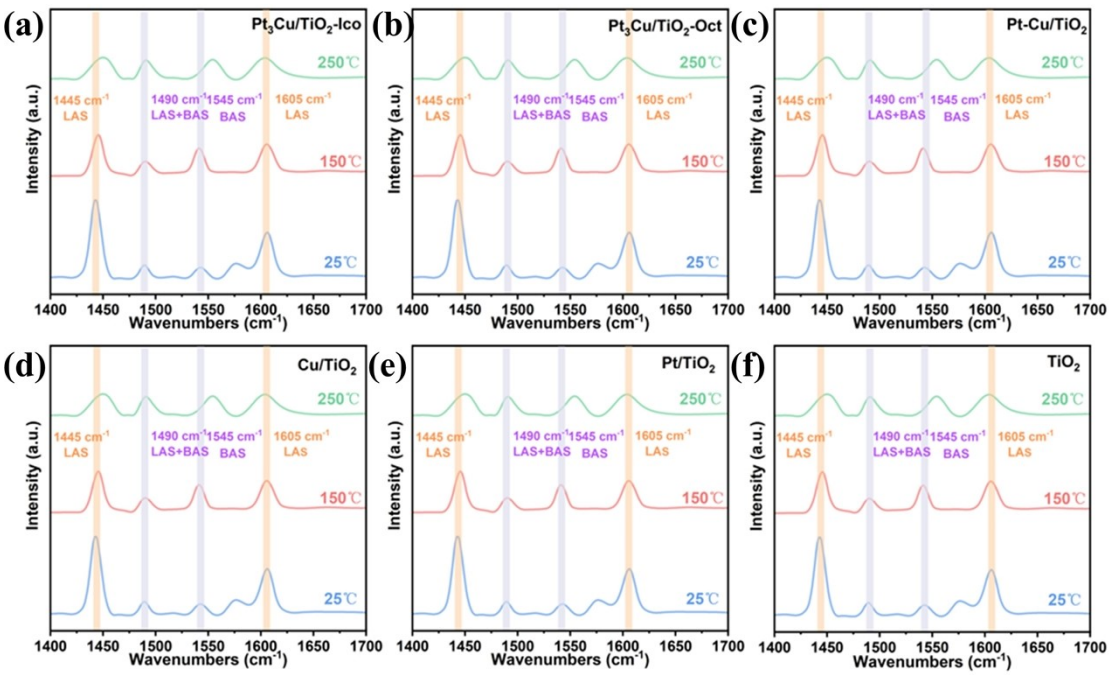

Fig. S6. Py-IR spectra at different temperatures.

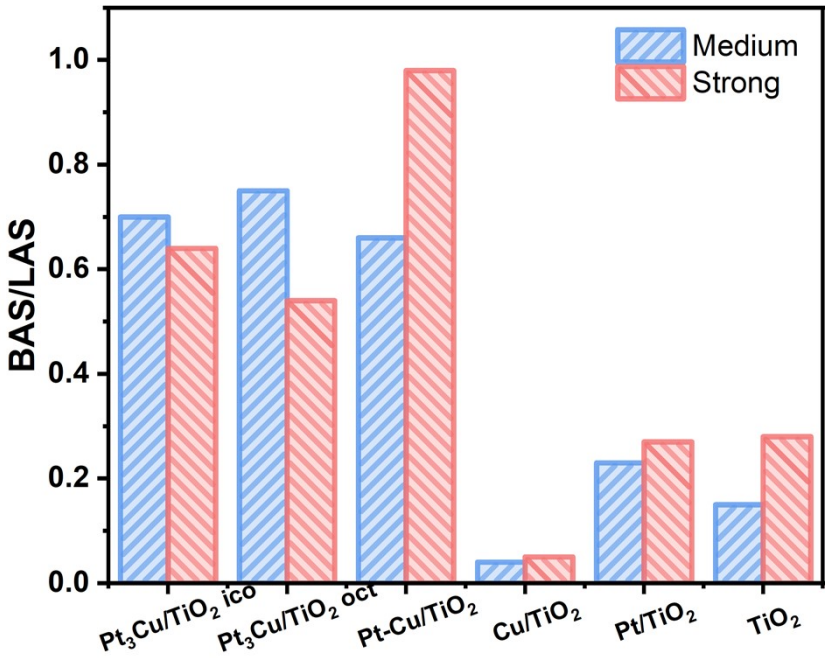

Fig. S7. BAS/LAS of the different catalysts.

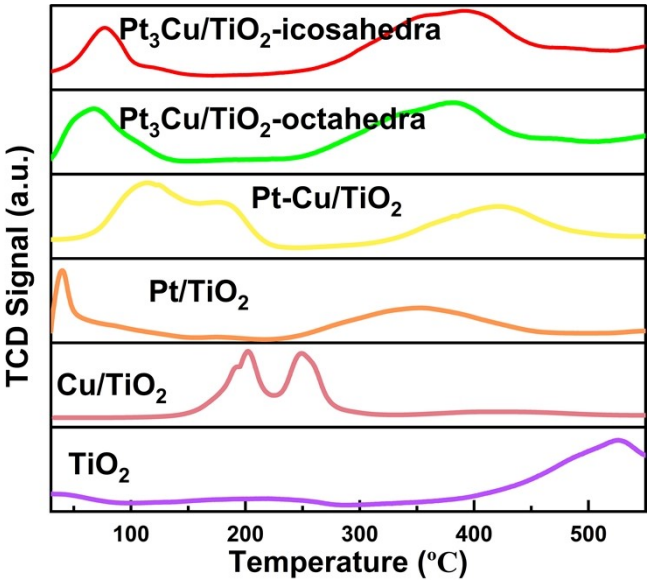

Fig. S8. H_2-TPR profiles of the catalysts.

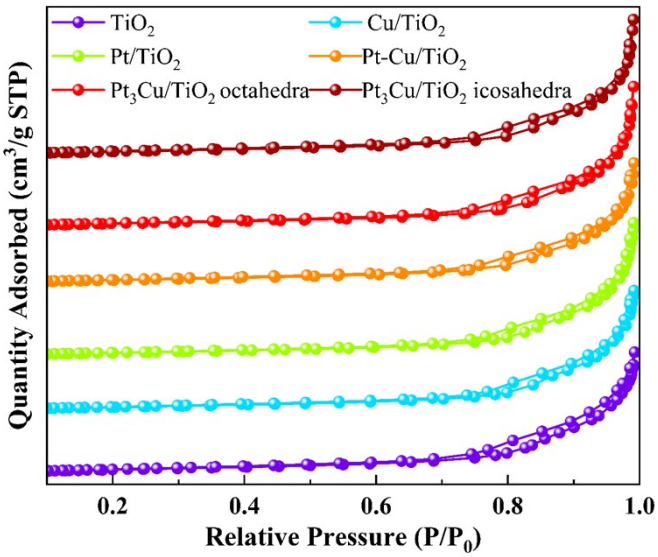

Fig. S9. N_2 adsorption-desorption

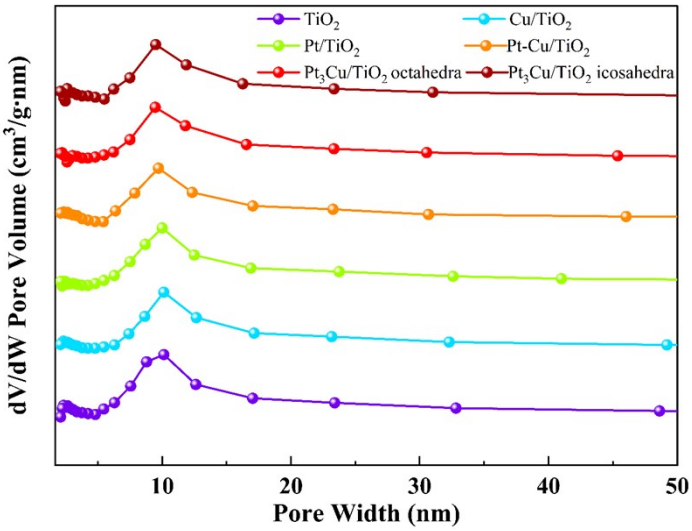

Fig. S10. Pore size distributions.

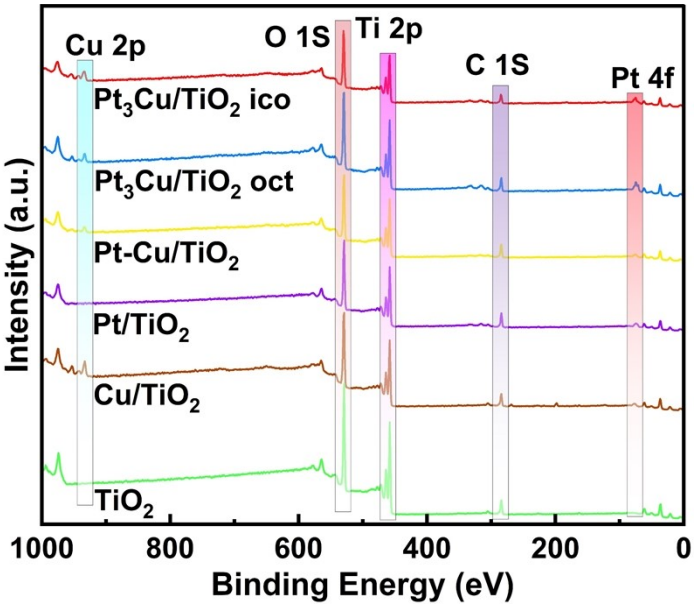

Fig. S11. XPS survey.

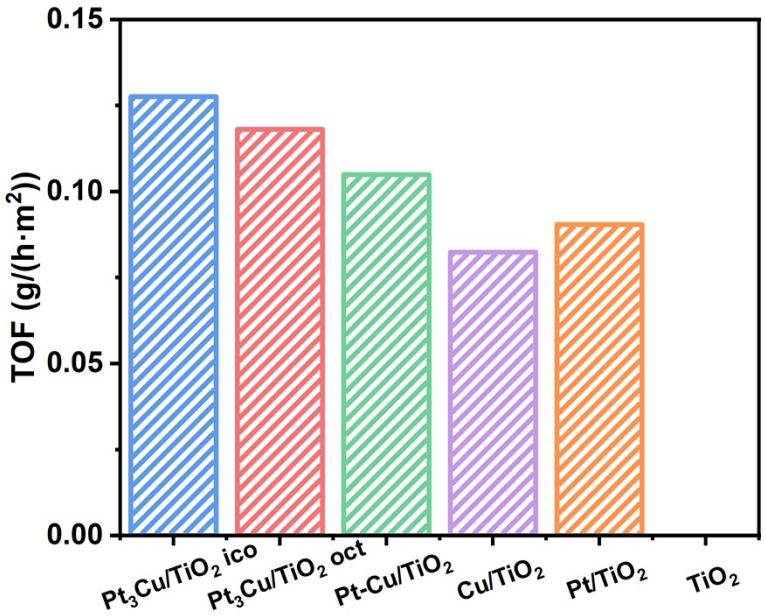

Fig. S12. TOF value of the catalysts.

Table S1. BAS and LAS contents of Py-IR.

Sample	Temperature	BAS content	LAS content	Total acid	BAS/LAS

	/°C	(μmol/g)	(μmol/g)	quantity (μmol/g)	
TiO_2	150	1.74	11.94	13.68	0.15
	250	0.96	3.46	4.42	0.28
Cu/TiO2	150	0.85	23.04	23.89	0.04
	250	0.64	11.93	12.57	0.05
Pt/TiO_2	150	5.68	24.69	30.37	0.23
	250	5.32	20.04	25.35	0.27
$Pt\text{-}Cu/TiO_2$	150	11.43	17.28	28.71	0.66
	250	7.99	8.20	16.19	0.96
Pt_3Cu/TiO_2 octahedra	150	14.89	19.79	34.68	0.75
	250	6.44	11.83	18.26	0.54
Pt_3Cu/TiO_2 icosahedra	150	15.11	21.57	36.67	0.70
	250	12.56	19.78	32.34	0.64

Table S2. Specific surface area and pore structure parameters of samples by N_2 adsorption-desorption curves.

Sample	Specific surface area /$m^2 \cdot g^{-1}$	Pore volume /$cm^3 \cdot g^{-1}$	Average pore size /nm
TiO_2	35	0.43	24.5
Cu/TiO2	62	0.44	14.5
Pt/TiO_2	64	0.46	12.9
Pt-Cu/TiO_2	63	0.44	14.0
Pt_3Cu/TiO_2 octahedra	63	0.51	12.7
Pt_3Cu/TiO_2 icosahedra	63	0.50	11.8

Table S3. Analysis of surface Pt species contents by XPS.

Sample	Pt species (%)	
	$Pt^0/(Pt^0+Pt^{2+})$	$Pt^{2+}/(Pt^0+Pt^{2+})$
Pt_3Cu/TiO_2 icosahedra	84.7	15.3
Pt_3Cu/TiO_2 octahedra	82.4	17.6
Pt-Cu/TiO_2	84.5	15.5
Pt/TiO_2	82.1	17.9

Table S4. Analysis of surface Cu species contents by XPS.

Sample	Cu species (%)	
	$Cu^0/(Cu^0+Cu^{2+})$	$Cu^{2+}/(Cu^0+Cu^{2+})$
Pt_3Cu/TiO_2 icosahedra	11.5	88.5
Pt_3Cu/TiO_2 octahedra	28.8	71.2
Pt-Cu/TiO_2	26.3	73.7
Cu/TiO_2	15.2	84.8

Table S5. Analysis of surface O species contents by XPS.

Sample	O species (%)		
	$O_L/(O_L+O_{V+}O_A)$	$O_V/(O_L+O_{V+}O_A)$	$O_A/(O_L+O_{V+}O_A)$
Pt_3Cu/TiO_2 icosahedra	74.6	9.2	16.2
Pt_3Cu/TiO_2 octahedra	76.1	9.1	14.8
Pt-Cu/TiO_2	85.3	7.8	7.9
Pt/TiO_2	69.3	9.0	21.7
Cu/TiO_2	67.4	8.8	23.8
TiO_2	76.5	7.2	16.3

Table S6. Structure parameters in the EXAF fitting of Cu K–edge and Pt L3–edge.

Sample	**Shell**	***N***	***R*(Å)**	**$\sigma^2(10^{-3}$ Å$^2)$**	**$\triangle E_0$ (eV)**	**amp**	***R* factor**
Cu–foil	Cu–Cu	12	2.54	8.5	3.32	1.018	0.0036
Pt_3Cu/C	Cu–Cu	4.2	2.53	9.9	7.87	1.018	0.027
	Cu-Pt	3.4	2.64	4.9	7.87	1.018	0.027
Pt–foil	Pt-Pt	12	2.76	4.5	8.21	0.893	0.003
Pt_3Cu/C	Pt-Cu	9.9	2.73	7.1	5.75	0.893	0.028

N: the coordination number. ***R***: the interatomic distance (bond length from center atom to coordination atom). **σ^2**: Debye–Waller factor to evaluate thermal and static disorder. **ΔE_0**: inner potential correction. **amp**: the amplitude reduction factor (amp=1.018 was determined by fitting EXAFS spectrum of Cu foil). ***R* factor**: the change of the interatomic distance relative to the initial length.

Table S7 The elemental analysis of the carbon deposition on the spent catalyst.

Sample	Element (wt.%)				
	C	O	Ti	Pt	Cu
Pt_3Cu/TiO_2 oct	21.46	53.885	20.826	1.3	2.529
Pt_3Cu/TiO_2 ico	11.61	64.824	22.368	0.308	0.89

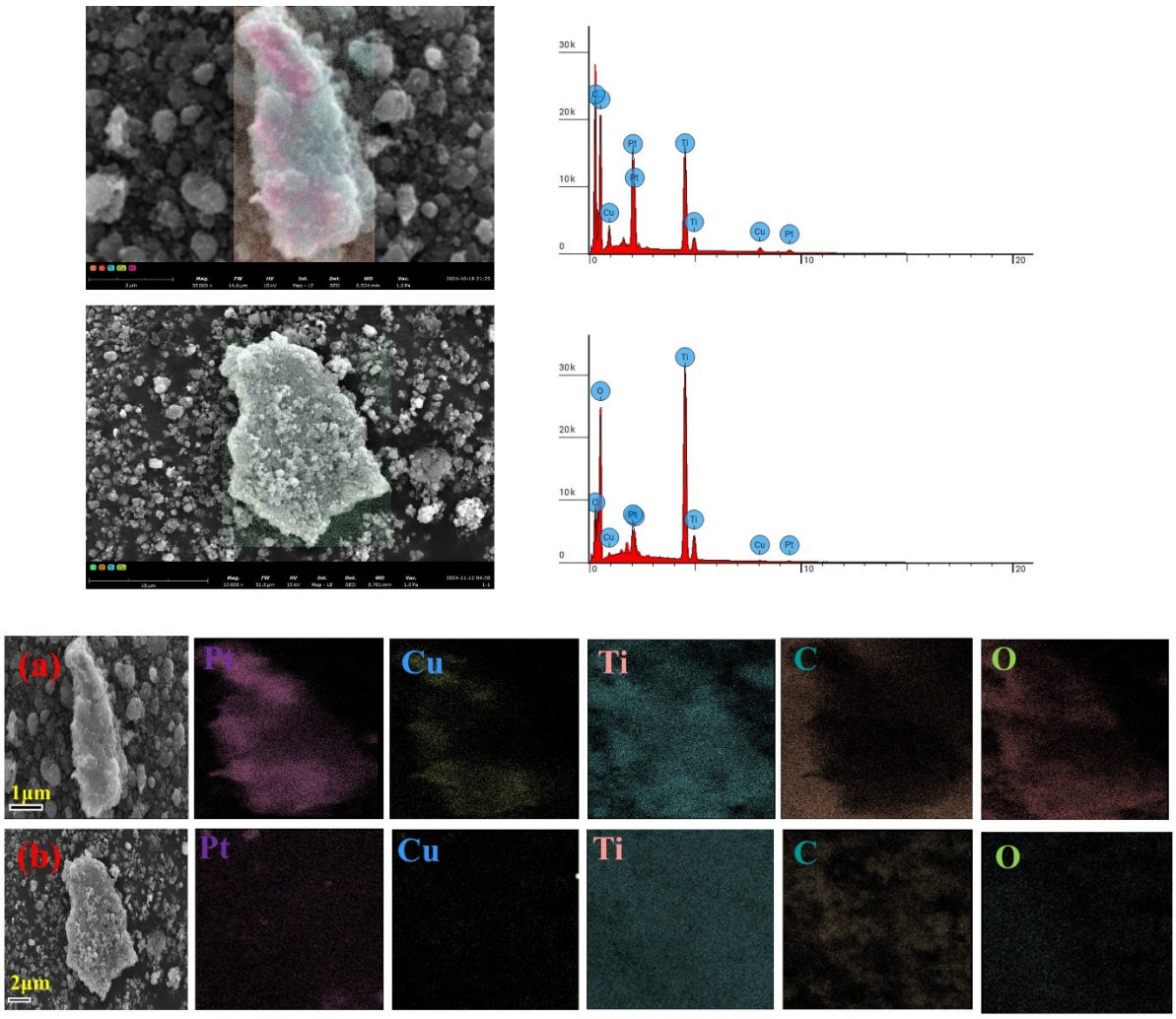

Fig. S13. SEM images of the spent catalysts.

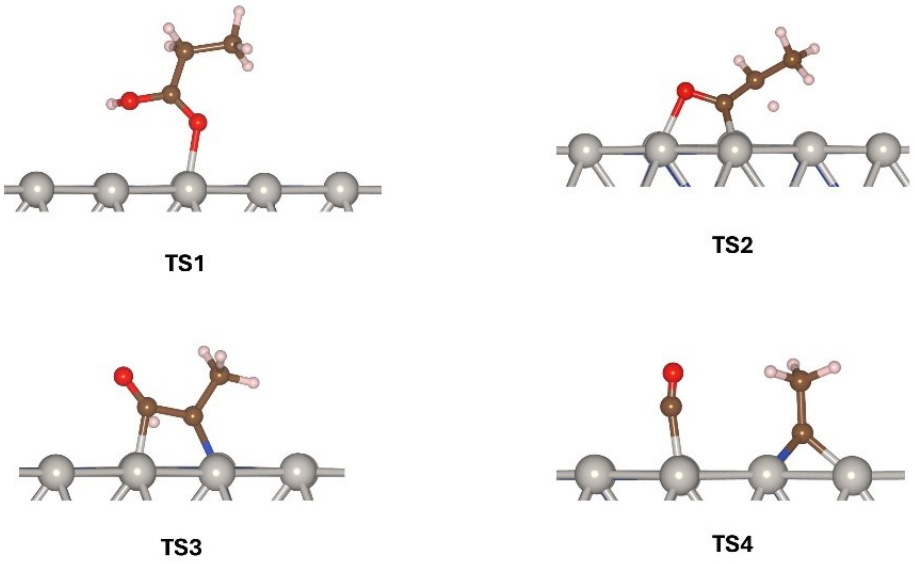

Fig. S14. Transition state.

Transition state:

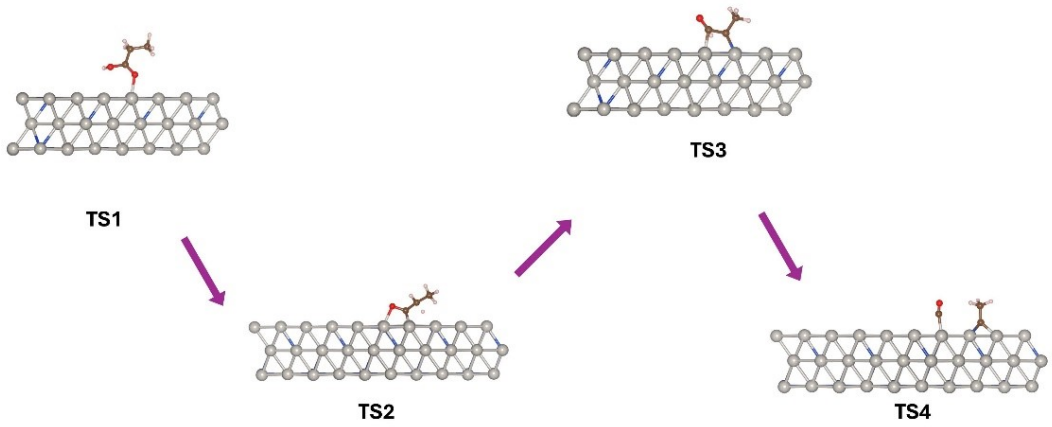

Fig. S15. Transition state.

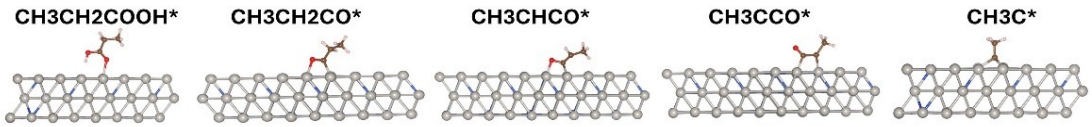

Fig. S16. Intermediate.